Journal of Molecular Structure 1229 (2021) 129842

Contents lists available at ScienceDirect

Journal of Molecular Structure

journal homepage: www.elsevier.com/locate/molstr

Synthesis, spectral characterization, crystal structure determination and antimicrobial activity of Ni(II), Cu(II) and Zn(II) complexes with the Schiff base ligand derived from 3,5-dibromosalicylaldehyde

Hadi Kargar[a,*], Amir Adabi Ardakani[b], Muhammad Nawaz Tahir[c], Muhammad Ashfaq[c], Khurram Shahzad Munawar[d,e]

[a] Department of Chemical Engineering, Faculty of Engineering, Ardakan University, P.O. Box 184, Ardakan, Iran
[b] Department of Chemistry, Ardakan Branch, Islamic Azad University, Ardakan, Iran
[c] Department of Physics, University of Sargodha, Punjab, Pakistan
[d] Department of Chemistry, University of Sargodha, Punjab, Pakistan
[e] Department of Chemistry, University of Mianwali, Mianwali, Pakistan

ARTICLE INFO

Article history:
Received 7 November 2020
Revised 15 December 2020
Accepted 22 December 2020
Available online 29 December 2020

Keywords:
Schiff base complexes
Spectral characterization
X-Ray structure
Antibacterial activity

ABSTRACT

Three new mononuclear metal complexes of the type M**L**, (M = Ni, Cu and Zn), with salen type tetradentate (ONNO) Schiff base, N,N′-bis(3,5-dibromosalicylidene)-1,3-diaminopropane (H_2**L**), have been prepared and characterized using FT-IR, ^{1}H NMR and elemental (CHN) analyses. In addition, the crystal structures of all complexes were analyzed by single crystal X-ray diffraction (SC-XRD) technique. The SC-XRD data explored that in the nickel and copper complexes a monoclinic crystal system was present and the coordination sphere around the metal centers consists of two oxygen atoms and two nitrogen atoms from chelating ligands to give a square planar geometry, while the zinc complex has orthorhombic crystal system and in addition to the atoms from chelating ligand, two O-atoms from the water molecules also coordinate to Zn atom to give distorted octahedral geometry. The *in vitro* antibacterial activities of the ligand and complexes were elaborated by screening them against Gram (+ve) (*Staphylococcus aureus* and *Bacillus cereus)* Gram (-ve) (*Escherichia coli* and *Pseudomonas aeruginosa).* All the synthesized compounds showed significant activity against the tested bacterial strains.

1. Introduction

The species having azomethine group make an excellent class of ligands which are matchless in their versatility, resemblance with natural biological molecules and have relevancy with metabolic processes taking place in biological systems [1]. The synthesis, spectral characterization and structure activity relationship of Schiff bases were studied in depth by numerous investigators previously [2–4]. The development of coordination chemistry by providing lone pairs from electron rich nitrogen and/or oxygen atoms to transition metals made them more interesting due to their physico-chemical, catalytic, photochromic, biological and therapeutic activities [5–10].

It was reported that salen type Schiff bases containing one or two halo-atoms in the aromatic rings have a broad range of applications [11–13]. The chelated Schiff bases containing N and O donor sites derived from halogenated salicylaldehyde were widely investigated due to their potential antitumor, antifungal and antibacterial activities [14–18].

Schiff bases complexes of Ni(II), Cu(II) and Zn(II) have distinctive properties and novel reactivity which serves as a base for the evolution of complex compounds for potential application in various fields [19,20]. These new and unusual properties open a new horizon to study their medical, analytical and biological prospects [21]. It is well known that several Schiff base complexes of Ni(II), Cu(II) and Zn(II) are used as anti-inflammatory, antipyretic, chemosensor, anti-diabetic, anti-bacterial, anti-cancer and anti-HIV (human immunodeficiency virus) [22–24].

In the present study tetravalent Schiff base ligand is selected on the basis of many reasons: a) single step preparation by the condensation of diamines with dibromo substituted salicylaldehydes; b) form effortlessly isolate able stable complexes with variety of metals; c) metal complexes display easily available axial Lewis acid sites for further coordination with either solvents of crystallization or with co ligands [25].

---

[*] Corresponding author.
E-mail addresses: h.kargar@ardakan.ac.ir, hadi_kargar@yahoo.com (H. Kargar).

https://doi.org/10.1016/j.molstruc.2020.129842
0022-2860/

In the current research we have focused our endeavor to the synthesis, structural elucidation and antimicrobial properties of bromo substituted salen type Schiff base and its complexes with Ni(II), Cu(II) and Zn(II).

2. Experimental

2.1. Physical measurements

Microanalysis of the complexes were done using a Heraeus CHN-O-FLASH EA 1112 elemental analyzer. FT-IR spectra were recorded on a FT-IR Prestige 21 spectrophotometer from 400-4000 cm^{-1} using KBr pellets. ^{1}H NMR spectroscopy in DMSO-d_6 (400 MHz, Bruker) was carried out by using tetramethylsilane (TMS) as internal standard. Chemical shifts for proton resonances are reported in ppm (δ) relative to tetramethylsilane and DMSO-d_6.

2.2. Synthesis of the Schiff base (H_2**L**)

All the chemicals and solvents used for the syntheses were of commercially available reagent grade and were used without further purification. Schiff base ligand was prepared following the literature procedure [26]. To a stirred ethanolic (25 mL) solution of 3,5-dibromosalicylaldehyde (2 mmol) was added an ethanolic (25 mL) solution of the 1,3-propanediamine (1 mmol). The reaction mixture was refluxed for 1-3 h in a water bath. The resulting solution was cooled to room temperature and the precipitates obtained were collected by suction filtration and washed with cold ethanol (3 × 10 mL) to afford the desired Schiff base.

2.3. General procedure for the synthesis of the complexes

In order to synthesize the nickel(II) complexes [Ni(**L**)], the metal precursor $Ni(OAc)_2.4H_2O$ (0.248 g, 1 mmol), for copper(II) complexes [Cu(**L**)], the metal precursor $Cu(OAc)_2.H_2O$ (0.200 g, 1 mmol), for zinc(II) complexes [Zn(**L**)], the metal precursor $Zn(OAc)_2.2H_2O$ (0.220 g, 1 mmol) was added to a hot methanolic solution (30 mL) of the corresponding ligand H_2**L** (1.0 mmol). The resultant mixture was refluxed for 3 h and then it was filtered, washed thoroughly with methanol and dried.

[Ni(**L**)], Yield: 81 %. Calculated for $C_{17}H_{12}Br_4N_2NiO_2$: C 31.19, H 1.85, N 4.28 %. Analysis found: C 31.31, H 1.92, N 4.17. FT-IR (KBr, cm^{-1}): υ C–H(aromatic): 3063, υ C–H(aliphatic): 2941, 2878, υ HC=N: 1618, υ C=C and C–N: 1578, 1508, 1442, 1375, υ C–O: 1319, υ Ni-N: 534, υ Ni–O: 415. ^{1}H NMR [d_6-DMSO, δ (ppm)]: 8.58 (s, 2 H, **H**–C=N), 7.58 (d, 2 H, J = 2.4 Hz, **H** arom.), 7.41 (d, 2 H, J = 2.4 Hz, **H** arom.), 3.73 (t, 4 H, C**H**$_2$-N), 2.08 (br, 2 H, C**H**$_2$-C).

[Cu(**L**)], Yield: 85 %. Calculated for $C_{17}H_{12}Br_4CuN_2O_2$: C 30.96, H 1.83, N 4.25 %. Analysis found: C 31.11, H 1.89, N 4.12. FT-IR (KBr, cm^{-1}): υ C-H(aromatic): 3064, υ C-H(aliphatic): 2941, 2868, υ HC=N: 1622, υ C=C and C–N: 1577, 1508, 1440, 1382, υ C-O: 1309, υ Cu–N: 545, υ Cu–O: 425.

[Zn(**L**)], Yield: 68 %. Calculated for $C_{17}H_{12}Br_4N_2O_2Zn$: C 30.88, H 1.83, N 4.24 %. Analysis found: C 30.97, H 1.92, N 4.02. FT-IR (KBr, cm^{-1}): υ C-H(aromatic): 3062, υ C-H(aliphatic): 2924, 2854, υ HC=N: 1620, υ C=C and C–N: 1575, 1508, 1440, 1384, υ C–O: 1298, υ Ni–N: 542, υ Ni–O: 410. ^{1}H NMR [d_6-DMSO, δ (ppm)]: 8.27 (s, 2 H, **H**–C=N), 7.63 (d, 2 H, J = 2.6 Hz, **H** arom.), 7.38 (d, 2 H, J = 2.6 Hz, **H** arom.), 3.77 (t, 4 H, C**H**$_2$-N), 1.97 (br, 2 H, C**H**$_2$-C).

2.4. Crystallographic methods

The X-ray diffraction measurement of Ni(**L**), Cu(**L**) and Zn(**L**) complexes were carried out on Bruker Kappa APEXII CCD X-ray diffractometer with graphite monochromated Mo-Kα radiation (λ = 0.71073 Å). The brown, dark red and yellow single crystals of Ni(**L**), Cu(**L**) and Zn(**L**) suitable for X-ray analysis were obtained from methanol solution and mounted on a glass fiber for data collection on Bruker Apex-II software [27]. The structures were solved by direct methods and subsequent difference Fourier maps on SHELXS97 [28] and then refined on F^2 by a full-matrix least-squares procedure using anisotropic displacement parameters. Atomic factors are from the international tables for X-ray Crystallography [29]. All non-hydrogen atoms were refined with anisotropic displacement parameters. Hydrogen atoms were placed in ideal positions and refined as riding atoms with relative isotropic displacement parameters. All refinements were performed using the SHELXL-2018/3 and WinGX-2014.1 programs [30,31]. The method to collect data was ω-scans and integrated using Bruker SAINT [32] software package. The crystallographic illustrations for complexes were prepared using ORTEP-3 [33] and platon [34]. Experimental parameters pertaining to single-crystal X-ray analysis of complexes are given in Table 1.

2.5. Antimicrobial activity

The Schiff base ligand and its metal(II) complexes were studied to assess their potentials as antibacterial agents. The tested microorganisms were the standard strains of two Gram-positive (*Staphylococcus aureus* PTCC1431, *Bacillus cereus* PTCC1015), and two Gram-negative (*Escherichia coli* PTCC1394, *Pseudomonas aeruginosa* PTCC1074) bacteria. In order to compare the results, erythromycin (15 mg/disk) was used as an antibiotic reference drug. The compounds were dissolved in DMSO at 50 μg/mL concentration. Determination of the antibacterial activity was carried out by spot-on the lawn method. Antibacterial activity of ligand and its corresponding complexes were tested by spotting the solution of 20 µL of ligand and its complexes onto the soft agar lawn, seeded with 10^7 cells/ml of *standard strains*. Each solution of ligand and its complexes were placed on the surface-inoculated TSA agars and incubated at 37°C for 24 h. Inhibition zone around the specimens was used to indicate antibacterial activity of each compound. Each test was performed in triplicate.

3. Results and discussion

3.1. Syntheses

The Schiff base ligand H_2**L** was prepared by the reaction of 1,3-diaminopropane with the corresponding 3,5-dibromosalicylaldehyde in nearly 78 % yield in ethanol. Treatment of the Schiff base ligands H_2**L** with the respective $Ni(OAc)_2.4H_2O$, $Cu(OAc)_2.H_2O$ and $Zn(OAc)_2.2H_2O$ in a 1:1 ratio under reflux condition led to the nickel(II), copper(II) and zinc(II) complexes, respectively. The spectroscopic data is in good agreement with the chemical formula proposed for Schiff base complexes. The synthetic procedure of Schiff base ligand and their complexes is presented in Scheme 1.

3.2. Crystal structures of complexes

In Ni**L** (Fig. 1, Table 1), the asymmetric unit consists of half of the molecule with nickel atom at the special position i.e. on two fold axis and the other half of the molecule is symmetrically generated with symmetry code (–x, -y,1/2-z). The coordination sphere around the Ni-atom consists of two oxygen atoms and two nitrogen atoms from chelating ligands. In the coordination sphere, the bond lengths Ni–O and Ni–N are 1.863 (2) and 1.879 (3) Å, respectively whereas the bond angles range from 84.69 (1)° to 92.00 (2)°, thus slightly distorted square planar geometry is formed. The 3-iminopropan-1-ol group A (C1/C6/C7/N1/O1)

Table 1
Crystal data and structure refinement parameters for complexes.

Identification code	Ni**L**	Cu**L**	Zn**L**
Chemical formula	$C_{17}H_{12}Br_4N_2NiO_2$	$C_{17}H_{12}Br_4CuN_2O_2$	$C_{17}H_{16}Br_4N_2O_4Zn$
Formula weight	654.60	659.47	697.33
Temperature (K)	296	296	296
Crystal system	Monoclinic	Monoclinic	Orthorhombic
Space group	*C2/c*	$P2_1/n$	*Pnma*
a (Å)	25.632(4)	13.975(2)	7.9472(3)
b (Å)	10.2255(14)	7.011(1)	24.5752(12)
c (Å)	6.9951(8)	19.961(3)	10.4656(4)
α (°)	90	90	90
β (°)	96.188(4)	109.459(4)	90
γ (°)	90	90	90
Volume (Å^3)	1822.7(4)	1844.0(5)	2043.97(15)
Z	4	4	4
Calculated Density (Mg/m^3)	2.386	2.375	2.266
Absorption coefficient (mm^{-1})	9.848	9.867	9.048
F(000)	1248	1252	1336
Crystal Shape	Needle	Rod	Block
Crystal color	Brown	Dark red	Yellow
Crystal size (mm)	0.35 × 0.14 × 0.12	0.46 × 0.26 × 0.24	0.36 × 0.22 × 0.18
Data Collection			
Absorption correction	multi-scan (SADABS; Bruker, 2005)	multi-scan (SADABS; Bruker, 2005)	multi-scan (SADABS; Bruker, 2005)
No. of measured, independent and observed [$I > 2s(I)$] reflections	7369, 1981, 1422	3637, 3637, 1731	9459, 2476, 1908
R_{int}	0.032	0.049	0.028
Theta range for data collection	1.598° to 27.000°	1.564° to 26.000°	2.115° to 27.923°
Index ranges	$-32\leq h\leq 32$, $-12\leq k\leq 13$, $-8\leq l\leq 5$	$-17\leq h\leq 16$, $-8\leq k\leq 8$, $-24\leq l\leq 24$	$-10\leq h\leq 10$, $-22\leq k\leq 32$, $-13\leq l\leq 9$
$(\sin\theta/\lambda)_{\max}$ (Å^{-1})	0.639	0.617	0.659
Refinement			
$R[F^2 > 2\sigma(F^2)]$, $wR(F^2)$, S	0.032, 0.054, 1.01	0.049, 0.126, 0.99	0.0289, 0.055, 1.01
No. of reflections	1981	3637	2476
No. of parameters	119	236	139
H-atom treatment	H-atom parameters constrained	H-atom parameters constrained	H-atoms treated by a mixture of independent and constrained refinement
$\Delta\rho_{\max}$, $\Delta\rho_{\min}$ (e Å^{-3})	0.43, −0.48	1.35, −1.35	0.42, −0.54

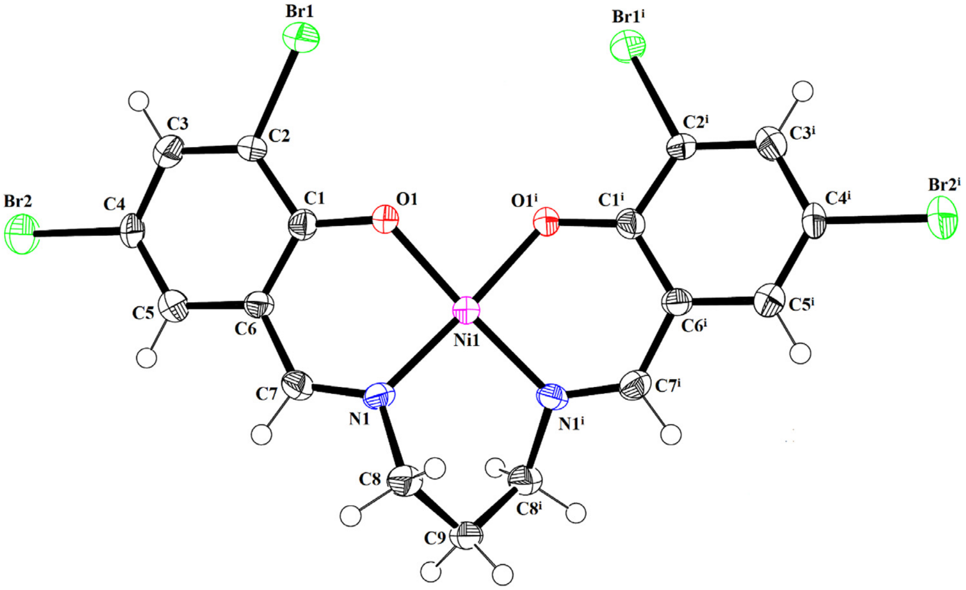

Fig. 1. ORTEP diagram of Ni**L** drawn at the probability level of 50%. H-atoms are shown by small circles of arbitrary radii.

and 3,5-dibromobenzene group B (C1-C6/Br1/Br2) are planar with r.m.s deviation of 0.0425 and 0.0454 Å, respectively. The C-atoms (C8/C9) are deviated by 0.4317 (5) and -0.6895 (6) Å above and below the plane of group A, respectively. The dihedral angle between A/B is 9.04 (6)°. Ring Puckering investigation shows that the chelating ring (C1/C6/C7/N1/O1/Ni1) has puckering amplitude Q = 0.388(2) Å, θ = 69.5(4)° and φ = 3.3 (5)°. It is also inferred that the ring (C8/C8^{i}/C9/N1/N1^{i}/Ni1) adopts T-form with puckering amplitude Q = 0.741(4) Å, θ = 90.0(2)° and φ = 270.0(2)°. The molecules are connected with each other through C–H···O bonding to form zigzag chains that run along the c crystallographic axis as shown in Figure S1 and given in Table 2. In addition to H-bonding, a weak interaction of type π-π stacking is found which helps in further stabilization of crystal packing. Benzene ring (C1-C6) located at the asymmetric position is involved in offset π-π stacking interaction with benzene ring located at (x,-y,-1/2+z) with inter-

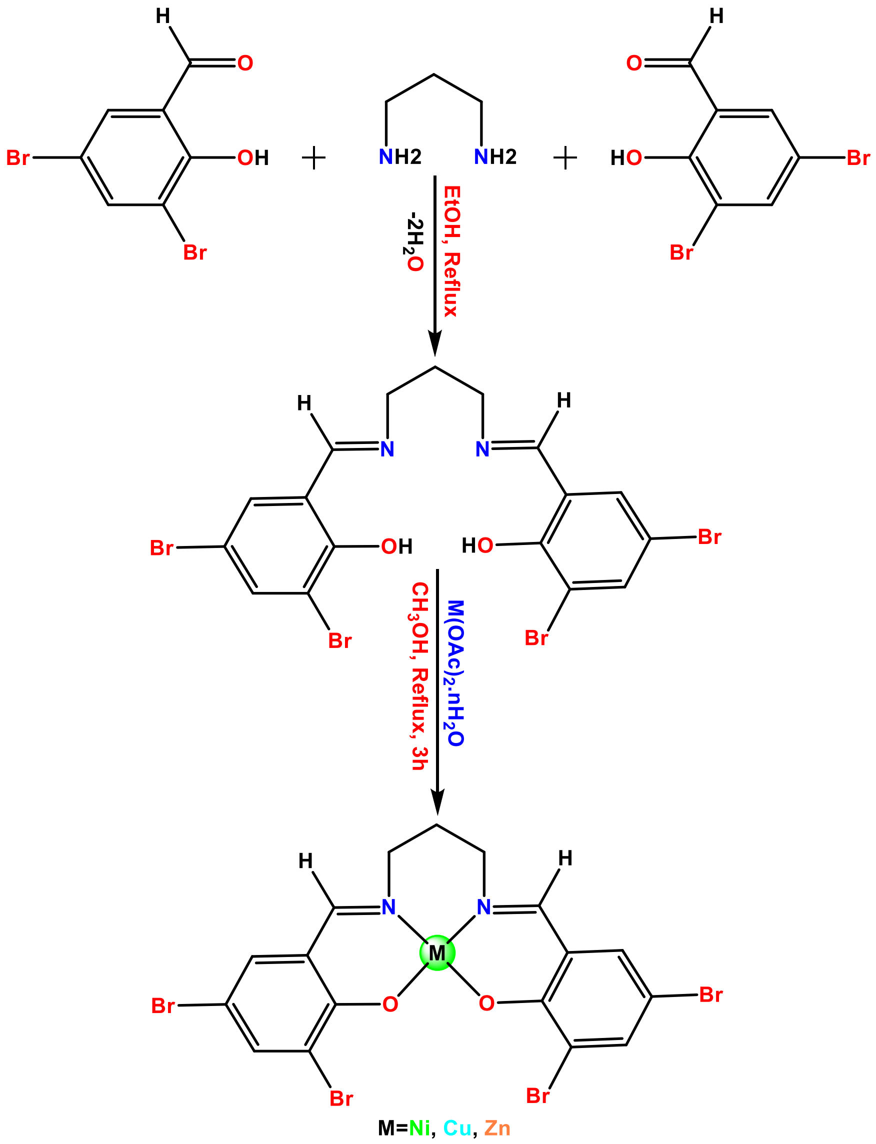

Scheme 1. The synthesis pathways of the ligand and its complexes.

Table 2
Hydrogen-bond geometry (Å, °) for complexes.

NiL	***D*—H•••*A***	***D*—H**	**H•••*A***	***D*•••*A***	***D*—H•••*A***
	C8—H8*B*••O1^{i}	0.97	2.65	3.315 (4)	126
	C8—H8*B*•••O1^{ii}	0.97	2.59	3.482 (4)	153
ZnL	***D*—H•••*A***	***D*—H**	**H•••*A***	***D*•••*A***	***D*—H•••*A***
	C8—H8*A*•••Br1^{ii}	0.97	2.99	3.781 (2)	140
	O2—H2•••Br1^{iii}	0.73 (2)	2.93 (3)	2.4312 (16)	128 (3)
	O2—H2•••O1^{iii}	0.73 (2)	2.18 (2)	2.862 (3)	155 (3)
	O3—H3*A*•••Br1^{iv}	0.72 (3)	3.08 (3)	3.5990 (17)	132 (3)
	O3—H3*A*•••O1 ^{iv}	0.72 (3)	2.17 (3)	2.804 (3)	148 (3)
CuL	***D*—H•••*A***	***D*—H**	**H•••*A***	***D*•••*A***	***D*—H•••*A***
	C3—H3•••Br3^{v}	0.93	3.09	3.955 (4)	155
	C8—H8*A*•••Br1^{vi}	0.97	3.11	3.867 (12)	136
	C8—H8***B*** •••O1^{vii}	0.97	2.55	3.459 (15)	155
	C9—H9*A*•••Br1^{vii}	0.97	3.04	3.750 (17)	131
	C9—H9*A*•••Br4^{vi}	0.97	3.03	3.711 (15)	129
	C9—H9*B*•••Br4^{viii}	0.97	2.86	3.670 (17)	141
	C10—H10*A*•••Br4^{vi}	0.97	3.07	3.823 (13)	135
	C10—H10*B*•••O2^{viii}	0.97	2.56	3.459 (15)	155
	C15—H15•••Br2^{ix}	0.93	3.09	3.935 (15)	152

Symmetry codes: (i) *x*, −*y*, *z*+1/2; (ii) −*x*, −*y*, −*z*+1; (ii) *x*, *y*, *z*−1; (iii) *x*+1/2, −*y*+1/2, −*z*+3/2; (iv) *x*−1/2, *y*, −*z*+3/2; (v) *x*−1/2, −*y*+1/2, *z*+1/2; (vi) *x*−1/2, −*y*+1/2, *z*−1/2; (vii) −*x*+1/2, *y*−1/2, −*z*+1/2; (viii) −*x*+1/2, *y*+1/2, −*z*+1/2; (ix) *x*+1, *y*, *z*.

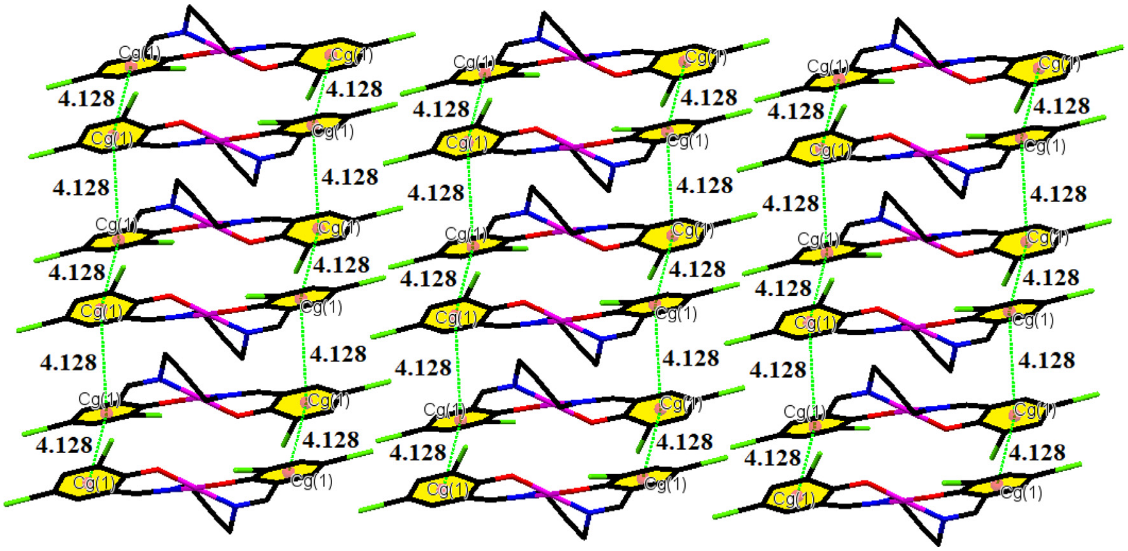

Fig. 2. Graphical representation of π-π stacking interaction for Ni**L**. Distance shown are measured in Å. H-atoms are not shown for clarity.

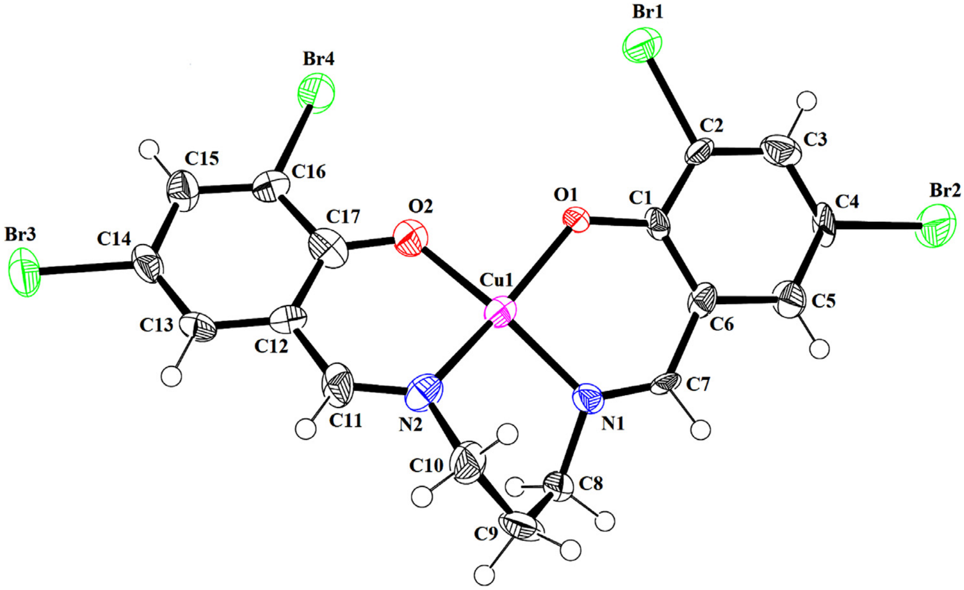

Fig. 3. ORTEP diagram of Cu**L** drawn at the probability level of 50%. H-atoms are shown by small circles of arbitrary radii.

centroid separation of 4.128 Å having ring-off of 2.648 Å. Similarly, benzene rings related by symmetry code (x,-y,1/2+z) are involved in off-set π-π stacking interaction with inter-centroid separation of 4.128 Å having ring-off of 1.998 Å as shown in Fig. 2.

In Cu**L** (Fig. 3, Table 1), the coordination sphere around the Cu-atom consists of two oxygen atoms and two nitrogen atoms from the chelating ligands. In coordination sphere, the bond lengths Cu–O1, Cu–O2, Cu–N1 and Cu–N2 are 1.891 (1), 1.908 (1), 1.949 (2) and 1.9732 (2) Å, respectively, whereas the bond angles range from 88.2 (4)° to 94.2 (5)°, thus slightly distorted square planar geometry is formed. In the first chelating ligand, the 3-iminopropan-1-ol group A (C1/C6/C7/N1/O1) and 3,5-dibromobenzene group B (C1-C6/Br1/Br2) are planar with r.m.s deviation of 0.0083 and 0.0119 Å, respectively. The C-atoms (C8/C9) are deviated by -0.2287 (2) and 0.9465 (2) Å below and above the plane of group A, respectively. The dihedral angle between A/B is 4.7 (3)° indicating that group A and B are almost parallel to each other. In the second chelating ligand, the 3-iminopropan-1-ol group C (C11/C12/C17/N2/O2) and 3,5-dibromobenzene group D (C12-C17/Br3/Br4) are planar with r.m.s deviation of 0.0177 and 0.0143 Å, respectively. The C-atom (C10) is deviated by 0.2135 (2) Å above the plane of group C, respectively. The dihedral angle between C/D is 4.1 (2)° indicating that group C and D are also almost parallel to each other. Ring Puckering investigation shows that the chelating ring (C8/C10/N1/N2/Cu1) has puckering amplitude Q = 0.761(12) Å, θ = 90.3(9)° and φ = 273.9(9)°. The molecules are connected with each other through C–H···O and C–H···Br bonding to form zigzag chains that run along b crystallographic axis as shown in Figure S2 and given in Table 2. In addition to H-bonding, a weak interaction of type π-π stacking is found which helps in further stabilization of crystal packing. π-π stacking interaction is found between different rings with inter-centroid distance ranges from 3.434 Å to 4.421 Å with slippage ranges from 0.540 Å to 2.987 Å as shown in Fig. 4.

In Zn**L** (Fig. 5, Table 1), the asymmetric unit consists of half of the molecule with zinc atom at the special position i.e. on two fold axis and the other half of the molecule is symmetrically generated with symmetry code (x,1/2-y,z). The coordination sphere

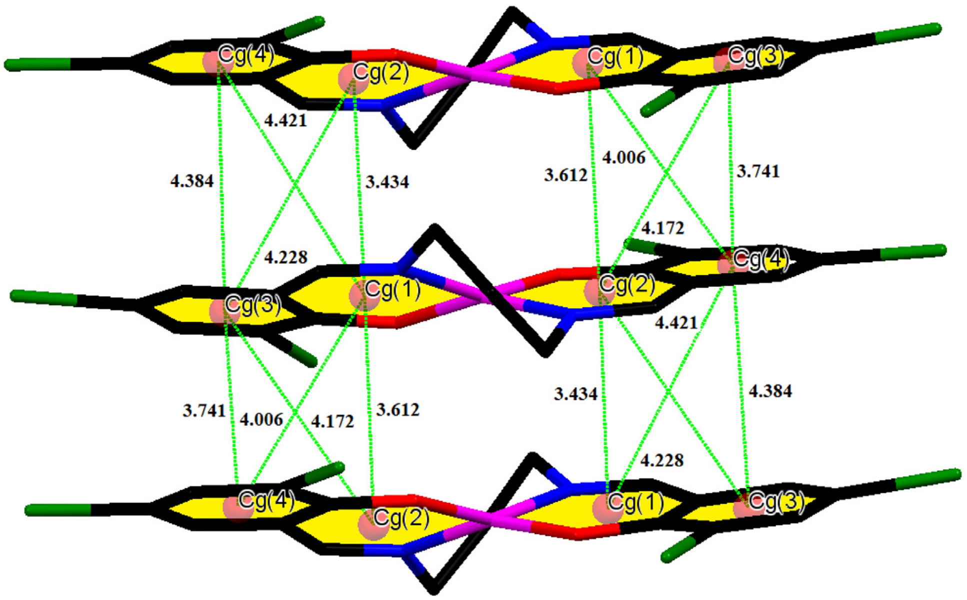

Fig. 4. Graphical representation of π-π stacking interaction for Cu**L**. Distance shown are measured in Å. H-atoms are not shown for clarity, where Cg(1), Cg(2), Cg(3), Cg(4) are the centroid of ring (C1/C6/C7N1/O1/Cu1), (C11/C12/C17/N2/O2/Cu1), (C1-C6), (C12-C17), respectively.

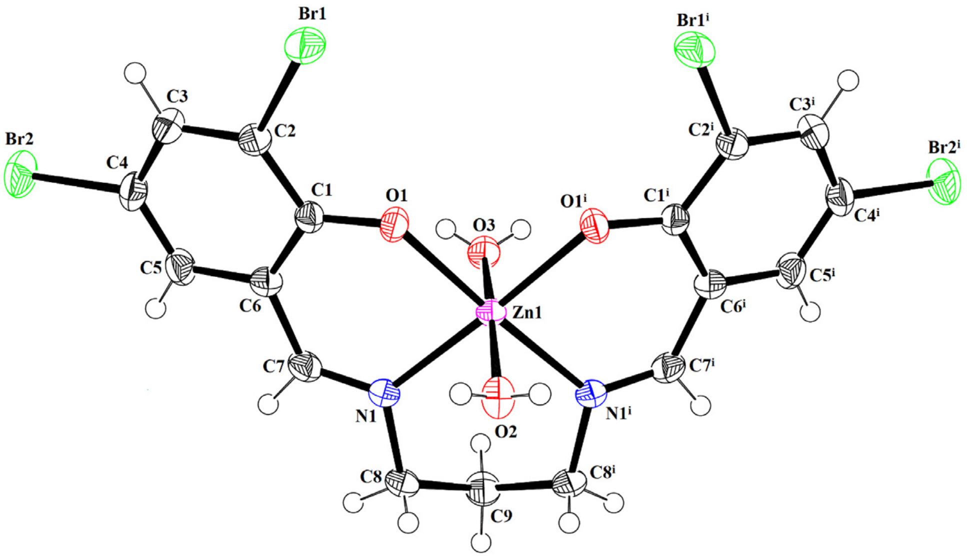

Fig. 5. ORTEP diagram of Zn**L** drawn at the probability level of 50%. H-atoms are shown by small circles of arbitrary radii.

around the Zn-atom consists of two oxygen atoms and two nitrogen atoms from chelating ligands and two O-atoms from the water molecules. In the coordination sphere, the bond lengths of Zn-O and Zn-N ranges from 2.0794 (2) to 2.1791 (3) Å and 2.1157 (2) to 2.1158 (2) Å, respectively. The bond angles range from 87.00 (7)° to 95.86 (8)°, bond lengths and bond angles are such that a slightly distorted octahedral geometry is formed. The 3-iminopropan-1-ol group A (C1/C6/C7/N1/O1) and 3,5-dibromobenzene group B (C1-C6/Br1/Br2) are planar with r.m.s deviation of 0.0238 and 0.0264 Å, respectively. The C-atoms (C8/C9) are deviated by 0.1903 (4) and -0.8298 (5) Å above and below the plane of group A, respectively. The dihedral angle between A/B is 4.7 (5)°. Ring Puckering investigation shows that the chelating ring (C1/C6/C7/N1/O1/Zn1) has puckering amplitude $Q = 0.3022(2)$ Å, $\theta = 64.6(4)°$ and $\varphi = 4.6$ (5)° whereas the ring (C8/C8^{i}/C9/N1/N1^{i}/Zn1) has puckering amplitude $Q = 0.535(3)$ Å, $\theta = 138.7(2)°$ and $\varphi = 360.0(4)°$. The molecules are connected with each other through O–H···O bonding to form one dimensional chain along [100] crystallographic direction, where OH is from water and acceptor O-atom is from 3-iminopropan-1-ol group as shown in Figure S3 and given in Table 2. In addition to H-bonding, a weak interaction of type π-π stacking is found which helps in further stabilization of crystal packing. Benzene ring (C1-C6) located at the asymmetric position is involved in offset π-π stacking interaction with benzene ring located at (1/2+x,y,3/2-z) and (-1/2+x,y,3/2-z) interaction with intercentroid separation of 3.963 Å having ring-off of 1.419 Å to 1.471 Å as shown in Fig. 6.

3.3. ^{1}H NMR spectra

^{1}H NMR spectra of the ligand was recorded in deuterated chloroform ($CDCl_3$), while the spectra of the complexes were recorded in DMSO-d_6. The ^{1}H NMR data of the metal complexes are given in the experimental section. In the ^{1}H NMR spectra of the H_2**L** signal at $\delta = 14.52$ ppm, which corresponds to the phenolic OH resonance is disappeared in the spectra of the nickel and zinc com-

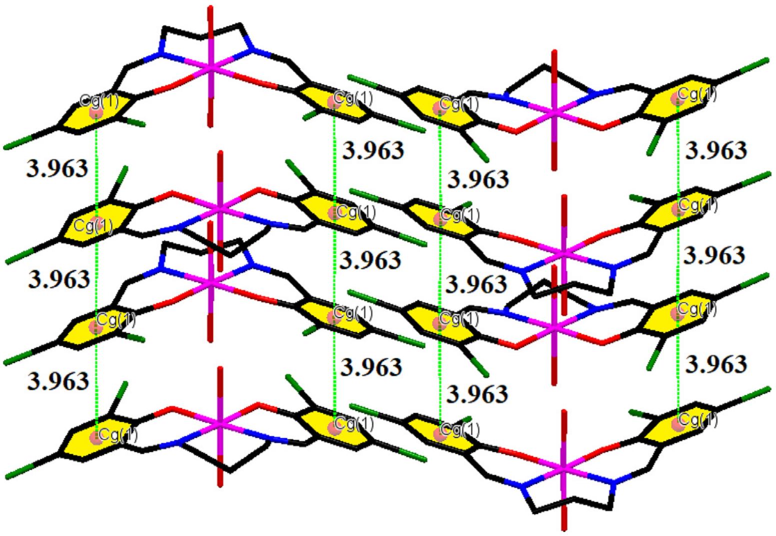

Fig. 6. Graphical representations of π-π stacking interaction for Zn**L**. Distances shown are measured in Å. H-atoms are omitted for clarity.

plexes (Figure S4). This clearly indicates that the Schiff base ligand is coordinated as an anionic ligand to the Ni(II) and Zn(II) ions. In the ^{1}H NMR spectra of the complexes, the signals at δ = 8.58, 8.27 ppm are attributed to the H–C=N- proton of imine, for nickel and zinc complex, respectively. There is a slight shift of the imine proton to down field in the obtained ^{1}H NMR spectra of the nickel and zinc complexes compared to the ligand one. This shift confirms the coordination of the phenolic oxygen and imine nitrogen to metal ions. The aromatic protons of the Ni(II) and Zn(II) complexes appear in the range of δ = 7.41–7.58 ppm and δ = 7.37–7.63 ppm, respectively. The –CH_2–N protons of the Ni**L** and Zn**L** complexes appear as a triplet at δ = 3.73 and 3.77 ppm, respectively. The broad signals at δ = 2.08 and 2.03 ppm are attributed to the –CH_2–C protons of the Ni**L** and Zn**L** complexes, respectively.

3.4. FT-IR spectra

The comparison between the selected bands in the FT-IR spectra of Schiff base ligand and its metal complexes are presented in Table 3 and Figure S5. In the FT-IR spectra of complexes, the ν (HC=N) and ν (C–O) bands shifted to lower and higher wavenumbers, respectively, in comparison with their corresponding free ligand thereby indicating a coordinative interaction between the iminic nitrogen and phenolic oxygen atoms with central metals. The iminic nitrogen and phenolic oxygen coordination could also be confirmed by the appearance of weak bands located at the low wavenumbers which are assigned to (M–N) and (M–O) at 530-545 cm^{-1} and 410-425 cm^{-1} respectively.

Table 3
FT-IR spectral data of ligand and its corresponding complexes (cm^{-1})

	H_2**L**	Ni**L**	Cu**L**	Zn**L**
υ(=CH)(aromatic)	3064	3062	3064	3062
υ(-CH)(aliphatic)	2943	2941	2941	2924
υ(HC=N)	1631	1618	1622	1620
υ(C–O)	1166	1319	1309	1298
υ(M–N)	-	534	545	542
υ(M–O)	-	415	425	410

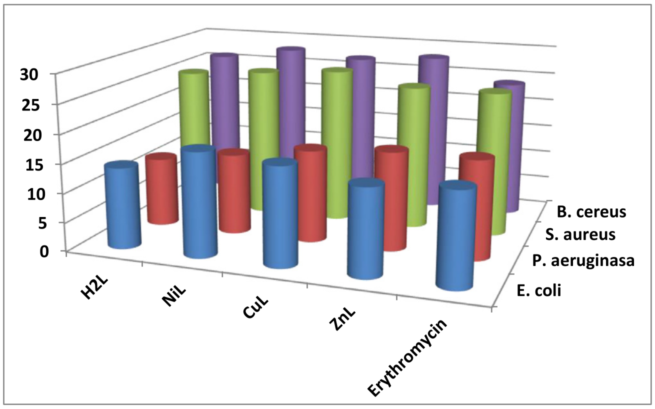

Fig. 7. A histogram shows the antibacterial evaluation of the investigated H_2**L** Schiff base ligand and its corresponding complexes.

3.5. Antibacterial activities

To contribute in the field of bioinorganic chemistry, all the compounds were screened for their antibacterial activity. Results have been recorded in the form of inhibition zones and activities are illustrated in Fig. 7. It has to be mentioned that DMSO did not exhibit any noticeable antibacterial activity, thus the solvent did not influence the biological activity of the studied compounds. On the basis of results, it is worth noting that: a) H_2**L** ligand showed the same antibacterial activity comparable to that of the standard. Further, the antibacterial activity of complexes may be significantly more to that of standards; b) The inhibition zones of the Schiff base ligand and corresponding complexes showed that the all compounds were more toxic towards gram positive strains. The reason is the difference in the structure of the cell walls. The cell membrane of the bacteria consists of peptidoglycan which is thicker in the gram positive bacteria [35]; c) On the basis of Overtone's concept [36] and tweedy's theory [37], metal ions play a significant role in enhancing the antibacterial activity on chelation [38]. However, in the present study the complexes are slightly more active than the free Schiff base ligand due the cell permeability. Another reason may be because of the lower lipophilicity the penetration of the complexes through the lipid membrane was decreased and, hence, they could neither block nor inhibit the growth of the microorganisms [39].

4. Conclusion

In summary, we have prepared a series of three novel metals complexes, Ni**L**, Cu**L** and Zn**L**, with a salen-type Schiff base derived by the condensation of 3,5-dibromosalicylidene and 1,3-diaminopropane by using alcohol as solvent. The synthesized complexes were characterized using various physico and spectrochemical techniques. Furthermore, the molecular structures of all complexes have been confirmed by single crystal X-ray diffraction. The results showed that the stoichiometry in complexes is 1:1 (ligand:metal). The coordination sites are azomethine nitrogens and phenolic oxygens as evident from ^{1}H-NMR and FT-IR. Only in the zinc complex the apical sites were involved in coordination with water molecules to increase the coordination number from four to six to make distorted octahedral geometry instead of square planar around the metal atom as confirmed by SC-XRD. The antibacterial screening tests disclosed that the number of live bacterial strains was greatly reduced after adding the complexes compared to free Schiff base ligand alone. The antibacterial data revealed that the toxicity of metal complexes towards gram positive strains is high relative to gram negative strains.

Author's statement

We would like to make a statement about the main contribution of authors: HK and AAA synthesized all the compounds, and characterized them by different techniques; AAA was responsible for biological data acquisition and analysis; MNT, MA and KSM collected the single-crystal X-ray diffraction data and determined the structures. HK wrote the manuscript with input from all authors. All authors discussed the results and commented on the manuscript.

Appendix A. Supplementary data

CCDC No. 2042418 (for Ni**L**), CCDC No. 2042419 (for Zn**L**) and CCDC No. 2042420 (for Cu**L**) contain the supplementary crystallographic data for this contribution. Copies of the data may be obtained free of charge on application to CCDC, 12 Union Road, Cambridge CB2 1EB, UK (Fax: +44-1223-336-033; E-mail: deposit@ccdc.cam.ac.uk or http://www. ccdc.cam.ac.uk).

Declaration of Competing Interest

The authors declare that they have no conflict of interest.

Acknowledgement

The support of this work by Ardakan University is gratefully acknowledged.

Supplementary materials

Supplementary material associated with this article can be found, in the online version, at doi:10.1016/j.molstruc.2020.129842.

References

[1] L.A. Saghatforoush, F. Chalabian, A. Aminkhani, G. Karimnezhad, S. Ershad, Synthesis, spectroscopic characterization and antibacterial activity of new cobalt (II) complexes of unsymmetrical tetradentate (OSN2) Schiff base ligands, Eur. J. Med. Chem. 44 (11) (2009) 4490–4495.

[2] L. Yun-Tong, D. Jing-Wen, L. Yao, G. Yi-Tong, S. Chao-Nan, L. Fu-Yao, X. Yu, J. Chang-Ling, Y. Zhong-Lu, Syntheses, Crystal Structures and Urease Inhibition of Two Manganesen (III) Complexes with Bis-Schiff Bases, Chinese J. Inorg. Chem. 34 (6) (2018) 1192–1198.

[3] V. Torabi, H. Kargar, A. Akbari, R. Behjatmanesh-Ardakani, H. Amiri-Rudbari, M.N. Tahir, Nickel(II) complex with an asymmetric tetradentate Schiff base ligand: synthesis, characterization, crystal structure, and DFT studies, J. Coord. Chem. 22 (2018) 3748–3762.

[4] A. Rauf, A. Shah, K.S. Munawar, S. Ali, M.N. Tahir, M. Javed, A.M. Khan, Synthesis, physicochemical elucidation, biological screening and molecular docking studies of a Schiff base and its metal (II) complexes, Arab, J. Chem. 13 (1) (2020) 1130–1141.

[5] H. Kargar, Synthesis, characterization and crystal structure of a manganese(III) Schiff base complex and investigation of its catalytic activity in the oxidation of benzylic alcohols, Transit. Met. Chem. 39 (2014) 811–817.

[6] K.S. Munawar, S. Ali, M.N. Tahir, N. Khalid, Q. Abbas, I. Qureshi, S. Shahzadi, Investigation of derivatized schiff base ligands of 1, 2, 4-triazole amine and their oxovanadium (IV) complexes: Synthesis, structure, DNA binding, alkaline phosphatase inhibition, biological screening, and insulin mimetic properties, Russ. J. Gen. Chem. 85 (9) (2015) 2183–2197.

[7] S. Chen, X. Liu, X. Ge, Q. Wang, Y. Xie, Y. Hao, Y. Zhang, L. Zhang, W. Shang, Z. Liu, Lysosome-targeted iridium (III) compounds with pyridine-triphenylamine Schiff base ligands: syntheses, antitumor applications and mechanisms, Inorg. Chem. Front. 7 (1) (2020) 91–100.

[8] H. Kargar, V. Torabi, A. Akbari, R. Behjatmanesh-Ardakani, A. Sahraei, M.N. Tahir, Synthesis, crystal structure, spectroscopic investigations and computational studies of Ni(II) and Pd(II) complexes with asymmetric tetradentate NOON Schiff base ligand, Struct. Chem. 30 (2019) 2289–2299.

[9] H. Kargar, V. Torabi, A. Akbari, R. Behjatmanesh-Ardakani, A. Sahraei, M.N. Tahir, Pd(II) and Ni(II) complexes containing an asymmetric Schiff base ligand: Synthesis, x-ray crystal structure, spectroscopic investigations and computational studies, J. Mol. Struct. 1205 (2020) 127642.

[10] J. Cisterna, V. Dorcet, C. Manzur, I. Ledoux-Rak, J.-R. Hamon, D. Carrillo, Synthesis, spectral, electrochemical, crystal structures and nonlinear optical properties of unsymmetrical Ni (II) and Cu (II) Schiff base complexes, Inorg. Chim. Acta 430 (2015) 82–90.

[11] K. Ansari, C. Lal, Synthesis, physicochemical properties and antimicrobial activity of some new benzimidazole derivatives, Eur. J. Med. Chem. 44 (10) (2009) 4028–4033.

[12] U. Böhme, B. Günther, Five and six-coordinate silicon complexes with an O, N, O′-chelating ligand derived from o-hydroxyacetophenone–N-(2-hydroxyethyl) imine, Inorg. Chem. Commun. 10 (4) (2007) 482–484.

[13] P. Noblía, M. Vieites, B.S. Parajón-Costa, E.J. Baran, H. Cerecetto, P. Draper, M. González, O.E. Piro, E.E. Castellano, A. Azqueta, Vanadium (V) complexes with salicylaldehyde semicarbazone derivatives bearing in vitro anti-tumor activity toward kidney tumor cells (TK-10): crystal structure of [VVO2 (5-bromosalicylaldehyde semicarbazone)], J. Inorg. Biochem. 99 (2) (2005) 443–451.

[14] A.N. Kursunlu, E. Guler, F. Sevgi, B. Ozkalp, Synthesis, spectroscopic characterization and antimicrobial studies of Co (II), Ni (II), Cu (II) and Zn (II) complexes with Schiff bases derived from 5-bromo-salicylaldehyde, J. Mol. Struct. 1048 (2013) 476–481.

[15] K.S. Munawar, S. Ali, M.N. Tahir, N. Khalid, Q. Abbas, I.Z. Qureshi, S. Hussain, M. Ashfaq, Synthesis, spectroscopic characterization, X-ray crystal structure, antimicrobial, DNA-binding, alkaline phosphatase and insulin-mimetic studies of oxidovanadium (IV) complexes of azomethine precursors, J. Coord. Chem. 73 (16) (2020) 2275–2300.

[16] K. Chichak, U. Jacquemard, N.R. Branda, The construction of (salophen) ruthenium (II) assemblies using axial coordination, Eur. J. Inorg. Chem. (2) (2002) 357–368 2002.

[17] Z. Lü, M. Yuan, F. Pan, S. Gao, D. Zhang, D. Zhu, Syntheses, crystal structures, and magnetic characterization of five new dimeric manganese (III) tetradentate Schiff base complexes exhibiting single-molecule-magnet behavior, Inorg. Chem. 45 (9) (2006) 3538–3548.

[18] V. Aomchad, S. Del Gobbo, P. Yingcharoen, A. Poater, V. D'Elia, Exploring the potential of group III salen complexes for the conversion of CO_2 under ambient conditions, Catal. Today (2020).

[19] E.M. Zayed, A.M. Hindy, G.G. Mohamed, Molecular structure, molecular docking, thermal, spectroscopic and biological activity studies of bis-Schiff base ligand and its metal complexes, Appl. Organomet. Chem. 32 (1) (2018) e3952.

[20] H. Kargar, R. Behjatmanesh-Ardakani, V. Torabi, A. Sarvian, Z. Kazemi, Z. Chavoshpour-Natanzi, V. Mirkhani, A. Sahraei, M.N. Tahir, M. Ashfaq, Novel copper(II) and zinc(II) complexes of halogenated bidentate N,O-donor Schiff base ligands: Synthesis, characterization, crystal structures, DNA binding, molecular docking, DFT and TD-DFT computational studies, Inorg. Chim. Acta 514 (2021) 120004.

[21] A.N. Kursunlu, E. Guler, F. Sevgi, B. Ozkalp, Synthesis, spectroscopic characterization and antimicrobial studies of Co (II), Ni (II), Cu (II) and Zn (II) complexes with Schiff bases derived from 5-bromo-salicylaldehyde, J. Mol. Struct. 1048 (2013) 476–481.

[22] Y. Luo, J. Wang, B. Zhang, Y. Guan, T. Yang, X. Li, L. Xu, J. Wang, Z. You, Syntheses, characterization and crystal structures of fluorine substituted Schiff base copper (II) and nickel (II) complexes with biological activity, J. Coord. Chem. 73 (12) (2020) 1765–1777.

[23] G.S. Huang, Y.M. Liang, X.L. Wu, W.M. Liu, Y.X. Ma, Some ferrocenyl Schiff bases with nonlinear optical properties, Appl. Organomet. Chem. 17 (9) (2003) 706–710.

[24] M. Aslantaş, E. Kendi, N. Demir, A.E. Şabik, M. Tümer, M. Kertmen, Synthesis, spectroscopic, structural characterization, electrochemical and antimicrobial activity studies of the Schiff base ligand and its transition metal complexes, Spectrochim. Acta, Part A 74 (3) (2009) 617–624.

[25] N. Noorussabah, M. Choudhary, N. Das, B. Mohan, K. Singh, R.K. Singh, K. Ahmad, S. Muhammad, S. Kumar, Copper (II) and Nickel (II) complexes of tridentate hydrazide and schiff base ligands containing phenyl and naphthalyl groups: synthesis, structural, molecular docking and density functional study, J. Inorg. Organomet. Polym. Mater. 30 (2020) 4426–4440.

[26] A.A. Ardakani, H. Kargar, N. Feizi, M.N. Tahir, Synthesis, characterization, crystal structures and antibacterial activities of some Schiff bases with N_2O_2 donor sets, J. Iran. Chem. Soc. 15 (2018) 1495–1504.
[27] APEX2, Bruker AXS Inc., Madison, Wisconsin, USA, 2013.
[28] G.M. Sheldrick, A short history of SHELX, Acta Crystallogr. A64 (2008) 112–122.
[29] W. Parrish, J. Langford, Kluwer, Dordrecht, 1992, pp. 48–50.
[30] G.M. Sheldrick, Crystal structure re finement with SHELXL, Acta Crystallogr. C71 (2015) 3–8.
[31] L.J. Farrugia, WinGX and ORTEP for windows: an update, J. Appl. Crystallogr. 45 (2012) 849–854.
[32] SAINT, Bruker AXS Inc., Madison, Wisconsin, USA, 2013.
[33] L.J. Farrugia, WinGX and ORTEP for Windows: an update, J. Appl. Cryst. 45 (2012) 849–854.
[34] A.L. Spek, Structure validation in chemical crystallography, Acta Crystallogr D65 (2009) 148–155.
[35] C. Mims, H.M. Dockrell, R.V. Goering, I. Roitt, D. Wakelin, M. Zuckerman, Medical Microbiology, 3rd edition, Elsevier Mosby, 2004 updated.
[36] Y. Anjaneyulu, R.P. Rao, Preparation, characterization and antimicrobial activity studies on some ternary complexes of Cu(II) with acetylacetone and various salicylic acids, Synth. React. Inorg. Met. Org. Chem. 16 (2) (1986) 257–2 72.
[37] B.G. Tweedy, Plant extracts with metal ions as potential antimicrobial agents, Phytopatology 55 (1964) 910–918.
[38] A. Sahraei, H. Kargar, M. Hakimi, M.N. Tahir, Distorted square-antiprism geometry of new zirconium (IV) Schiff base complexes: synthesis, spectral characterization, crystal structure and investigation of biological properties, J. Mol. Struct. 1149 (2017) 576–584.
[39] A. Sahraei, H. Kargar, M. Hakimi, M.N. Tahir, Synthesis, characterization, crystal structures and biological activities of eight-coordinate zirconium(IV) Schiff base complexes, Transit. Met. Chem. 42 (2017) 483–489.